Article

The Dirac fermion of a monopole pair (MP) model

Samuel. P. Yuguru[1]

1. Chemistry Department, School of Natural and Physical Sciences, University of Papua New Guinea, P. O. Box 320, Waigani Campus, National Capital District 134, Papua New Guinea, Tel. : +675 326 7102; Fax. : +675 326 0369;

Email address: samuel.yuguru@upng.ac.pg.

Abstract

The electron of magnetic spin −1/2 is a Dirac fermion of a complex four-component spinor field. Though this is effectively addressed by relativistic quantum field theory, an intuitive form of the fermion still remains lacking. In this novel undertaking, the fermion is examined within the boundary posed by a recently proposed MP model of a hydrogen atom into 4D space-time. Such unorthodox process somehow is able to remarkably unveil the four-component spinor of non-abelian in both Euclidean and Minkowski space-times. Supplemented by several postulates, the relativistic and non-relativistic applications of the magnetic spin property are explored from an alternative perspective. The outcomes have important implications towards an alternative interpretation of quantum electrodynamics and a probable quantum universe, where quantum mechanics and general relativity are expected to merge. Such findings could pave the paths for future pursuits of physics beyond the Standard Model and they warrant further investigations.

Keywords: Dirac fermion; magnetic spin; 4D space-time; quantum universe; Standard Model

1. Introduction

At the fundamental level of matter, particles are described by wave-particle duality, charges and their spin property. These properties are revealed from light interactions and are pursued by the application of relativistic quantum field theory. The theory of special relativity defines lightspeed to be constant in a vacuum and the

Preprints (www.preprints.org) | NOT PEER-REVIEWED | Posted: 22 November 2022 doi:10.20944/preprints202210.0172.v3

rest mass of particles as, $m = E/c^2$. By definition, the particle-like property of light waves are massless photons possessing spin 1 of neutral charge. Any differences to the spin, charge and mass-energy equivalence provide the inherent properties of the particles at the fundamental level and this is termed causality. Based on quantum field theory, particles are considered as fields permeating space at less than lightspeed, where there is a level of indetermination towards unveiling their charge and spin property, while the wave property is depended on the instrumental set-up. Such definition counteracts the deterministic viewpoint of non-relativistic Schrödinger wave function, ψ, which is extremely useful in describing precisely the probability of future events for a lone particle such as an electron in orbit of the atom [1]. First, it does not account for the spin property of the particles. Second, the ψ is classically applied to physical waves such as for the water waves. Thus, it is difficult to imagine wavy form of particles freely permeating space without interactions and this somehow collapses to a point at observation [2].

At the atomic state, the energy is radiated in discrete energy forms in infinitesimal steps of Planck's radiation, $\pm h$. Such interpretation is consistent with observations except for the resistive nature of proton decay [3]. Despite such set-back, the preferred quest is to make non-relativistic equations become relativistic due to the shared properties of both matter and light at the fundamental level as mentioned above.

Beginning with Klein-Gordon equation [4], the energy and momentum operators of Schrödinger equation,

$$\hat{E} = i\hbar\frac{\partial}{\partial t}, \qquad \hat{p} = -i\hbar\boldsymbol{\nabla}, \tag{1}$$

are adapted in the expression,

Preprints (www.preprints.org) | NOT PEER-REVIEWED | Posted: 22 November 2022 doi:10.20944/preprints202210.0172.v3

$$\left(\hbar^2\frac{\partial^2}{\partial t^2} - c^2\hbar^2\boldsymbol{\nabla}^2 + m^2c^4\right)\psi(t,\bar{x}) = 0. \quad (2)$$

Equation 2 incorporates special relativity, $E^2 = p^2c^2 + m^2c^4$ for mass-energy equivalence, $\boldsymbol{\nabla}$ is the del operator in 3D space, $\hbar$ is reduced Planck constant and i is an imaginary number, $i = \sqrt{-1}$. Only one component is considered in Equation 2 and it does not take into account the negative energy contribution from antimatter. In contrast, the Hamiltonian operator, $\hat{H}$ of Dirac equation [5] for a free particle is,

$$\hat{H}\psi = (-i\boldsymbol{\nabla}.\boldsymbol{\alpha} + m\beta)\psi. \quad (3)$$

The ψ has four-components of fields with vectors of momentum, $i\nabla$ and gamma matrices, $\alpha.\ \beta$ represent Pauli matrices and unitarity with m equal to particle mass. The concept is akin to, $e^+ e^- \longrightarrow 2\gamma$, where the electron annihilates with its antimatter to produce two gamma rays. Antimatter existence is observed in Stern-Gerlach experiment and positron from cosmic rays. While the relativistic rest mass is easy to grasp, how fermions acquire mass other than Higgs field remains yet to be solved at a satisfactory level [6]. But perhaps, the most intriguing dilemma is offered by the magnetic spin ±1/2 of the electron and how this translates to a Dirac fermion of a four-component spinor. Such a case remains a very complex topic, whose intuitiveness in terms of a proper physical entity remains lacking. In this novel undertaking, the electron is examined within the boundary posed by a recently proposed MP model of 4D space-time of a hydrogen atom. With this process, the transition of the electron to a Dirac fermion is unveiled. Supplemented by a number of postulates, the fermion's relationships to both relativistic and non-relativistic aspects of the spin property are examined within

the context of current knowledge. Such outcomes demonstrate the dynamics of the model, where its compatibility to a quantum universe and quantum field theory is presented. These findings if considered, could pave alternative paths for the pursuits of physics beyond the Standard Model and they warrant further investigations.

2. Dirac fermion of a MP model

An intuitive conversion of the electron to a Dirac fermion of four-component spinor field by Lorentz transformation in Euclidean space-time of non-abelian is presented in Fig. 1a. In Fig. 1b, Minkowski space-time for the fermion of spin ±1/2 in superposition states is offered. From these illustrations, a number of postulates are drawn from the first principle of space-time.

1) A lone electron within the MP model is likened to Bohr model of the hydrogen atom (Fig. 1a). Its circular orbit is transformed to an ellipsoid of a MP field of magnetic field, **B** and it is dissected perpendicularly by a circular electric field, **E**, that appears to be a straight line to render its dipole moment. Precession of the MP field of a clock face generates a 4D space-time. The electron's orbit of time reversal due Einsteinian gravity is quantized by Bohr orbits (BOs) in degeneracy into *n*-dimensions. The cyclic BO in Euclidean space-time (e.g., positions 1 and 5 in Fig. 1a) is transformed to angular momentum in Minkowski space-time (Fig. 1b). Such pairings offer local entanglement in violation of lightspeed of spherical rotation. The spacing between the BOs of *n*-dimensions is defined by *h* with unitarity, λ sustained. Its excitation with external light interaction assumes, $E =$

Preprints (www.preprints.org) | NOT PEER-REVIEWED | Posted: 22 November 2022 doi:10.20944/preprints202210.0172.v3

nhv, whereas the probability of locating the electron is defined by De Broglie relationship, $\lambda = h/p$. Multiple MP fields are assumed for electrons distribution in multielectron atoms.

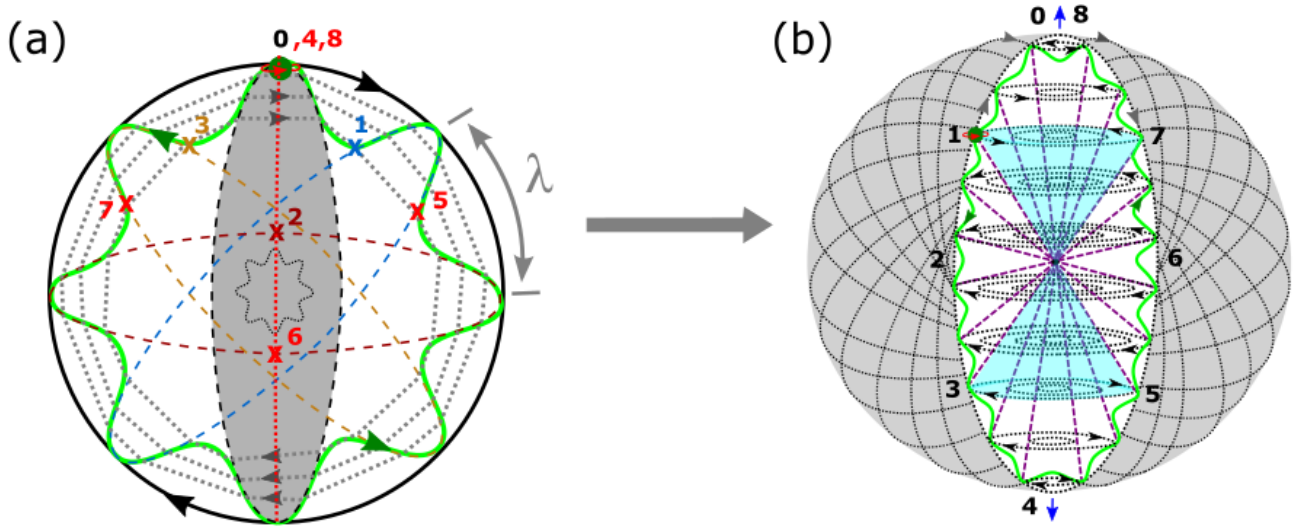

Figure 1. The MP field of an electron-wave diffraction. Image adapted from ref. [7]. (a) A spinning electron's (green dot) orbit of time reversal due to gravity is transformed to an ellipsoid of a MP field (grey area) and its precession into 4D space-time is of a clock face (black and grey arrows). To *an external observer* at an inertia frame of reference, the electron pops in and out of existence at positions, 0, 1, 2, 3 in repetitive process of a clock face by their respective colored MP fields for a 360° rotation to produce a positron. The process is attained at 180° spherical rotation of a hemisphere. The complete spherical rotation at 360° corresponds to 720° rotation, where the electron is restored to its original position. At positions, 0, 4 and 8, maximum twists and unfolding process begins comparable to both Dirac belt trick [8] and Balinese cup trick [9]. In this case, the circular electric field appears to be a straight line (red dotted) and this dissects the monopole field to generate its dipole moment. The area defined by the shift in the electron's positions is of non-abelian Euclidean lattice within a hemisphere, whereas the sphere identifies with Euclidean space-time. (b) The MP field (white area) at position 1 is projected along the vertical axis for an electron cloud model. Minkowski space-time is applicable to *an internal observer* positioned at the center, where the pairings of 1, 5 and 3,7 of the BOs (a)

Preprints (www.preprints.org) | NOT PEER-REVIEWED | Posted: 22 November 2022 doi:10.20944/preprints202210.0172.v3

translate to a pair of light-cones (navy colored) with their Dirac matrices given by, $\gamma^{1,3}$. Inversion of symmetry through the center violates parity, whereas chirality and time reversal symmetry are conserved. Orthogonal projection of chirality, $\frac{1}{2}(1 \pm i\gamma^0\gamma^1\gamma^2\gamma^3)$ with respect to the electron's path is reduced to spin, $\frac{1}{2}(1 \pm i\gamma^1\gamma^3)$ for the quantized states of BOs (*Postulate 1*). The superscripts represent Dirac matrices such that 0 is equal to positions 4 and 8, 1 to 5, 2 to 6 and 3 to 7 of time invariance for local realism and entanglement. In Hilbert space, the spin angular momentum of the orbit (purple dotted lines) is projected towards singularity at the center. Its outward projection relates to the precession of the overarching MP field. ***E*** of a straight path is assumed by the arrow of time of a light-cone in asymmetry of unidirectional and this translates to a magnetic dipole moment (blue arrows) of the MP field. In this way, Schrödinger's electron field, ψ is transformed to a Dirac fermion of a four-component spinor field, $i\gamma^0\gamma^1\gamma^2\gamma^3$. Thus, once maximum twists are attained along the BOs by the electron's orbit, the unfolding process begins at positions 0, 4 and 8 and this somehow resembles both Dirac belt trick [8] and Balinese cup trick [9].

2) The orthogonal relationship between **E** and **B** further implies that the precessing MP field of a clock face (Fig. 1a) would be a straight line dissecting a spherical electric field by reciprocity (Fig. 2a). The electron path is then composed of both *u*- and *v*-type particle- like properties in Hilbert space with precession at lightspeed. Parity transformation from positions 0 to 4 and then 4 to 8 completes the cyclic rotation of the electron on a straight path. The probability of locating the electron anywhere at positions 0 to 8 in Hilbert space is Hermitian by the orthogonal relationship, $P(0\rightarrow8) = \int_\tau \psi^* \hat{H} \psi d\tau$, with τ is time and $\hat{H}$

Preprints (www.preprints.org) | NOT PEER-REVIEWED | Posted: 22 November 2022 doi:10.20944/preprints202210.0172.v3

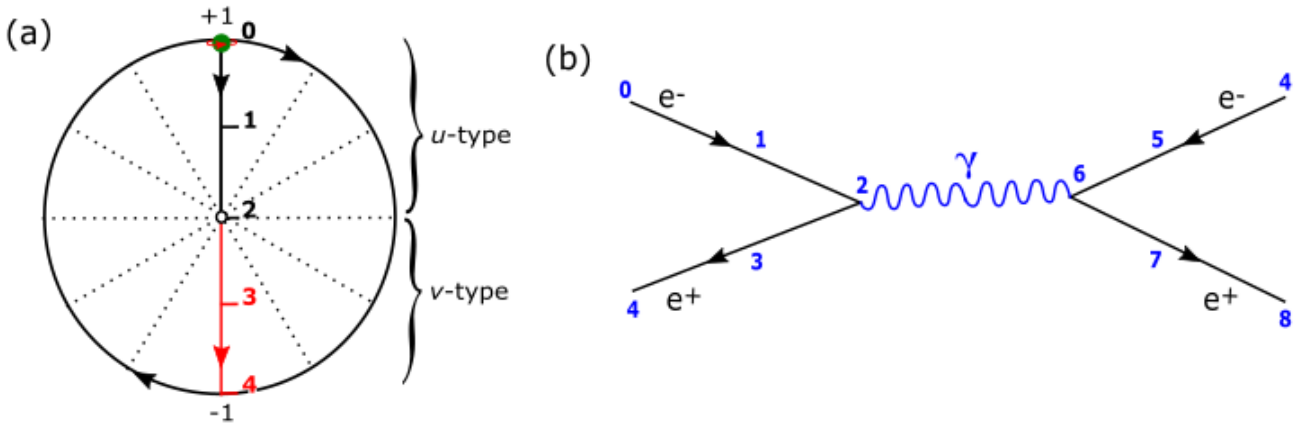

Figure 2. Orthogonal relationship of magnetic and electric fields of the MP model. (a) The electron's orbit of time reversal (Fig. 1a) is aligned on a straight path in perpendicular to a circular electric field. With spherical rotation, the electron's path constitutes both *u*- and *v*- type particle-like properties in Hilbert space. The precessing MP field of a clock face is polarized, ±1 in accordance with the shift in the electron's position. The process is reversed by parity transformation from position 4 to 8 for a cyclic magnetic field on a straight path in repetitions (i.e., mimicking a 360° rotation compared to 180° spherical rotation of a hemisphere for the electric field). Maximum twists and unfolding process resembling Dirac belt trick occur at positions, 0, 4 and 8 in repetitions. These interpretations are captured by a Feynman diagram of electron-positron pair (b).

is the Hamiltonian operator. These descriptions are captured by a Feynman diagram of positron-electron pair (Fig. 2b), where the unfolding process occurs at positions 0, 4 and 8 after maximum twists assumed along BOs analogous to Dirac belt trick. The electron path defined by h (*Postulate 1*) is transformed to $\hbar$ by the orthogonal duality of **E** and **B** (Fig. 1a and 2a). This sustains the unitary of the gauge field defined by the "natural units", $\hbar = c = 1$ with its rotation assumed in accordance with Euler's formula, $e^{i\pi} + 1 = 0$ due to the orthogonality of **E** and **B**. Thus, the electron's position is defined by $i\hbar$ and this further incorporates the uncertainty principle, $\Delta E.\Delta t \geq \hbar/2$ or $\Delta x.\Delta p \geq \hbar/2$ of

Preprints (www.preprints.org) | NOT PEER-REVIEWED | Posted: 22 November 2022 doi:10.20944/preprints202210.0172.v3

time invariance. In this way, the (hydrogen) atom is conserved while radiation by $\hbar$ in accordance with the 2nd law of thermodynamics is of linear time (Fig. 3a, b and c).

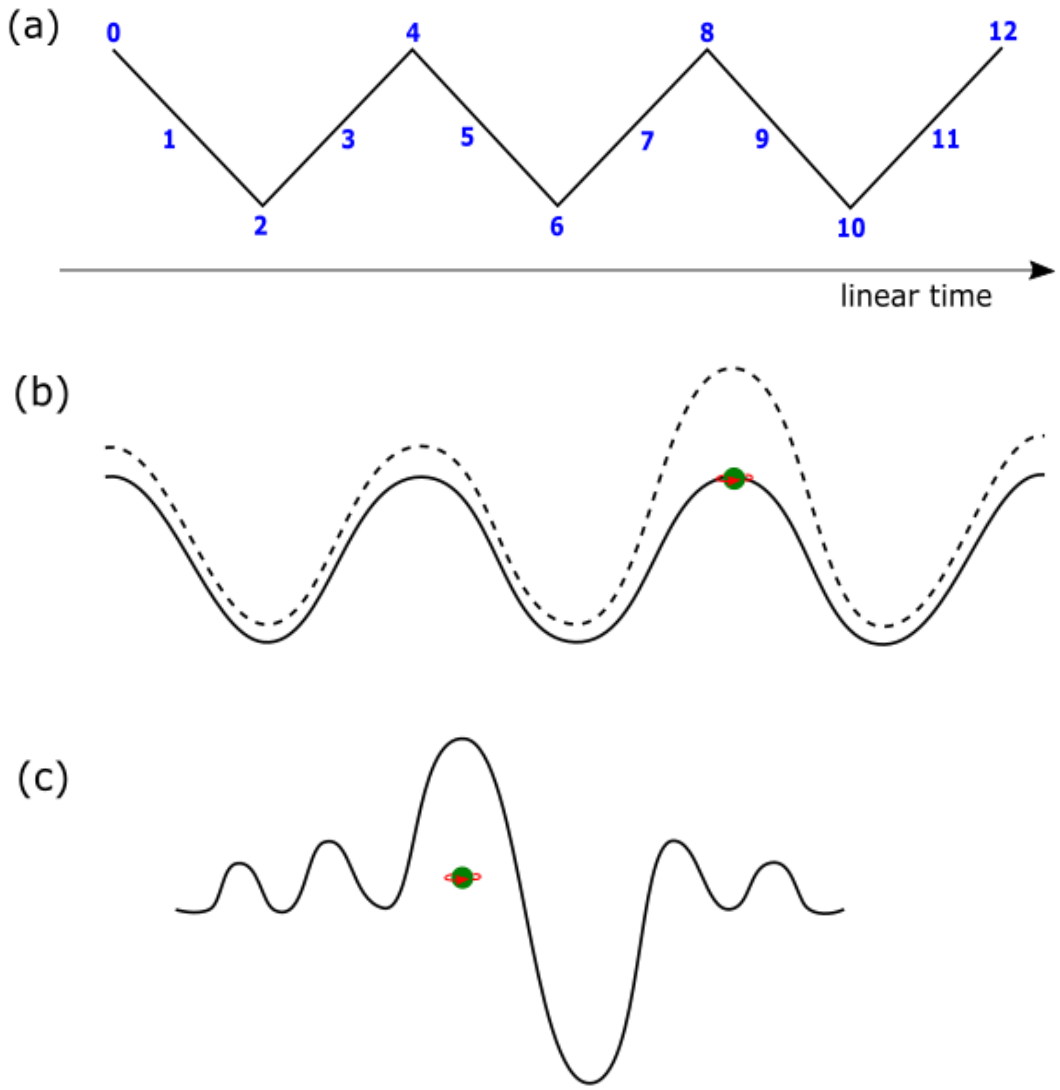

Figure 3. Induction of electromagnetic waves from the MP model into space. (a) The magnetic field assumed at positions 0 to 4 (e.g., Fig. 2a) is accompanied by the electric field of a hemisphere at spherical rotation of 180°. The numbered positions from 9 onwards repeat the process described by positions 0 to 8 of the MP model (Fig. 1a). (b) The corresponding sinusoidal wave of the radial distribution is energized by the presence of the electron (dotted wavy curve).

Preprints (www.preprints.org) | NOT PEER-REVIEWED | Posted: 22 November 2022 doi:10.20944/preprints202210.0172.v3

Its dissipation into space could resemble sea waves losing energy into open space while the atom is conserved. (c) The angular distribution is also applicable to the electron path on a straight line (e.g., Fig. 2a).

3) At 360° rotation, Dirac four-component spinor, $\psi = \begin{pmatrix} \psi_0 \\ \psi_1 \\ \psi_2 \\ \psi_3 \end{pmatrix}$ assumes their own antimatter at positions, 0, 1, 2 and 3 of the BOs (Fig. 1a and b). Only two positions ψ_1 and ψ_3 generate observable light-cones (Fig. 1b) for the intrinsic spin, ±1/2 property and are connected by a geodesic curve of a close loop mimicking the BO. The outcome of each spin is determined by Born's probabilistic interpretation,$|\psi|^2$, where the past or future paths of the electron from 0 to infinity are not accounted for at observations.
4) In a multiverse of the models at a hierarchy of energy scales, the procession ensues in the following manner, nucleus => atom => planet => star => galaxy. There is obvious distinction to matter between the scales such as life on Earth and gluons at the nucleus. However, the underlying energy scale is possibly dictated by the MP model. In this case, the electron to atom is comparable to satellite to planet, planet to star and possibly star to galaxy. Whether these explanations could accommodate the basic principles of general relativity is open to further discussions. For example, gravitational time dilation is applicable in Hilbert space (Fig. 2a), gravitational lensing to the shifts in the orthogonal relationship between **E** and **B** of the MP model (e.g., Fig. 1a and 2a), perihelion precession to precessing MP field of a clock face (Fig. 1a) and so forth.
5) If time of a clock face resembles the precession of the MP field into 4D space-time (Fig. 1a and 2a), it should tick faster in the atom due to the scale and this progresses slower towards the higher hierarchy of scales in a multiverse consistent with the twin paradox narrative. Thus, an observer on

 doi:10.20944/preprints202210.0172.v3

Earth is subject to an electron cloud model of the atom (Fig. 1a and 2a) and redshift in the sun's precession about the Milky Way. In this case, the cosmic microwave background of a MP field type and its precession is expected to be considerably redshifted of linear time (e.g., Fig. 3a) to an observer on Earth in an accelerated frame of reference [7]. Thus, Clausius's conservation of energy for the universe is assumed, where entropy is recycled in a multiverse by the application of 2nd law of thermodynamics at reduced rate towards the higher hierarchy of scales.

6) The non-relativistic Schrödinger ψ is assigned to the electron or its particle-hole symmetry. Its relativistic transformation to Dirac fermion within the MP model is attained in both Euclidean and Minkowski space-times (Fig. 1a and b). Observation of a monopole field of an oscillator type is restricted by an overriding hologram so it becomes difficult to isolate monopoles from the MP field.

These postulates with respect to the unveiled Dirac fermion of four-component spinor field are tantamount to the tenets of physics. How these become relevant to both relativistic and non-relativistic interpretations of the electron field, ψ of the hydrogen atom are further explored in this study with some of their implications discussed. The outcomes are expected to offer new insights to existing knowledge in physics from an alternative perspective.

3. Consolidation of the model

The spin property alluded within the MP model and the offered postulates are explored for their applicability to quantum physics. First, the limitations to the applications of quantum field theory are briefly discussed. Next, the model's relevance to both quantum mechanics and relativity is elucidated by including some

 doi:10.20944/preprints202210.0172.v3

examples of observational scenarios. In the final section, the implications to high-energy physics, general relativity and Dirac spinor are expounded by assuming a quantum universe in a multiverse of the models at a hierarchy of energy scales.

3.1 Limitations of quantum field theories (QFTs)

QFT considers matter to be made up of fields at the fundamental level. Electromagnetism, gravity, weak and strong nuclear forces permeate these fields and are mediated by the particle types known as the bosons of 0 to ±1 charges and spin 1. Only gravity is mediated by the boson type called the graviton of spin 2. The quanta of the fields resemble particle-like property of spin 1/2 with variable charges and these are termed fermions. Light-matter (or particles) interactions induce vacuum fluctuations and polarizations, where virtual particles pop in and out of existence. The above processes are captured well by Feynman diagrams and are adapted into QFT such as quantum electrodynamics. The theory has seen a tremendous success to account for light interactions with atoms such as the splitting of hydrogen spectral lines to fine structure. However, there are two major limitations to such approach. First, a complex task of renormalization is normally done by computation to constrain the effects of particles' self-interactions via virtual photons exchanges in order to conform to measurements. The process defeats the heuristic rule of naturalness [10] and brings into question what the approximate physical structure of matter at the fundamental level is like. Second, gravity warps the fabric of space-time based on the theory of general relativity. Its quantization as a force is yet to be defined without gravitons observed in experiments conducted so far. Other physics phenomena constrained by the application of QFTs include, neutrino mass, matter-antimatter asymmetry, dark matter, dark energy and so

Preprints (www.preprints.org) | NOT PEER-REVIEWED | Posted: 22 November 2022 doi:10.20944/preprints202210.0172.v3

forth. For these reasons, the MP model offers an alternative path to the interpretation of the Dirac fermion and its spin property (Fig. 1a and b). How this relate to the electron, ψ and hence, hydrogen atom is further explored in this section.

3.2 Non-relativistic aspects of the hydrogen atom

The electron in orbit resembles the Bohr model of the hydrogen atom, whereas its translation to 4D space-time is of Dirac fermion (Fig. 1a; *Postulate 1*). Its non-relativistic Schrödinger field, ψ in 3D space is defined by the spherical polar coordinates, Ω, Φ, θ with respect to the Cartesian coordinates, *x*, *y*, *z* (Fig. 4). The angular component is assigned to the BO and this is defined by θ and Φ within a cylindrical boundary. The radial component into *n*-dimension is referenced to the *z*-axis. The configurations of ψ due to the precession of the MP field is defined by Ω of a von Neumann entropy state (Fig. 4). The microcanonical ensemble for the entropy, $S = k\ In\ \Omega$ is applicable to the model, with *k* providing an approximation of the exponential rise in the quantized states of the fermion in Hilbert space (Fig. 2a, b and 3a). The precession of the spherical model then assumes the integrals [11],

$$\int_0^{\infty}\int_0^{\pi}\int_0^{2\pi} f(r)r^2 sin\theta dr d\theta d\phi = \int_0^{\infty} f(r)4\pi r^2 dr. \quad (4)$$

where the polar coordinates for the axes are, $x = rsin\theta cos\phi$, $y = rsin\theta sin\phi$ and $z = rcos\theta$ (Fig. 4). The shift in the position of the electron during orbit is defined by $\hbar$ and it is also

Preprints (www.preprints.org) | NOT PEER-REVIEWED | Posted: 22 November 2022 doi:10.20944/preprints202210.0172.v3

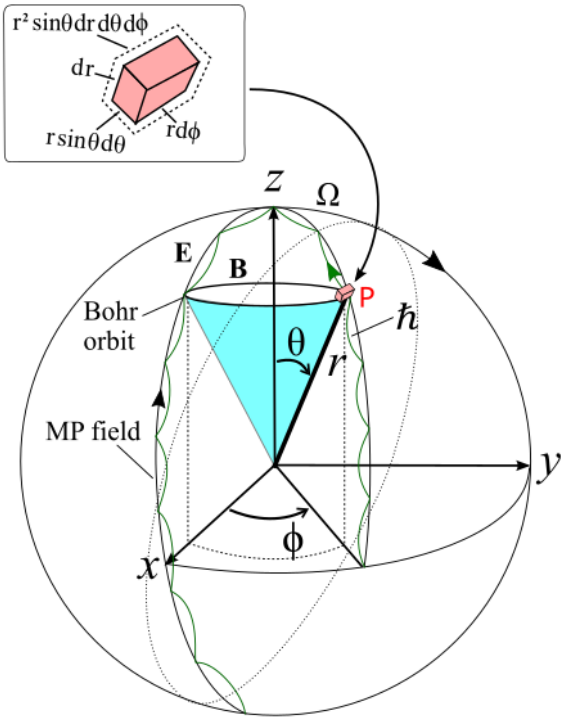

Figure 4. Deterministic harmonic oscillation (green wavy curve) of Schrödinger Ψ within the MP field (see also Fig. 1b). The polar coordinates are referenced to the center. Image modified from ref. [11].

applicable to the Dirac fermion (Fig. 1a; *Postulate 2*). Thus, $i\hbar$ for the particle obeys the Euler's form, $\Psi^{i\theta} = cos\theta + i\,sin\theta$. Its evolution with time adheres to the general non-linear Schrödinger's equation,

$$i\hbar\frac{\partial\psi}{\partial t}(x,t) = \hat{H}\psi\,(x,t). \qquad (5)$$

Equation 5 is first order in space-time and is applicable to Equation 3, with indeterminacy in the spin property offered by the Dirac fermion in 4D space-time (Fig. 1b) and this somehow obeys the Schrödinger cat narrative. Infinitesimal radiation defined by $\hbar$ is accorded to the 2nd law of thermodynamics (*Postulate 2*). The $\Psi_{n,l,m,ms}$ incorporates the principal quantum number (n), angular momentum quantum number (l), magnetic quantum number (m) and magnetic spin (m_s). How these aligned with observations is examined next.

3.3 Relativistic transformation of the hydrogen atom

Preprints (www.preprints.org) | NOT PEER-REVIEWED | Posted: 22 November 2022 doi:10.20944/preprints202210.0172.v3

Much of the data generated for the atom or its quantum state with theoretical applications due to light-matter interactions involve relativistic interpretations. In this case, the Schrödinger electron field, ψ in Hilbert space (Fig. 4) is transformed to four-component spinor field of the Dirac fermion in Euclidean space-time within a hemisphere with an overarching hemisphere of

the MP field forming a hologram (Fig. 1a) of gauge invariance. Actual measurement is reduced to 1D space of linear time as a function of traversing electromagnetic waves along straight paths. These explanations

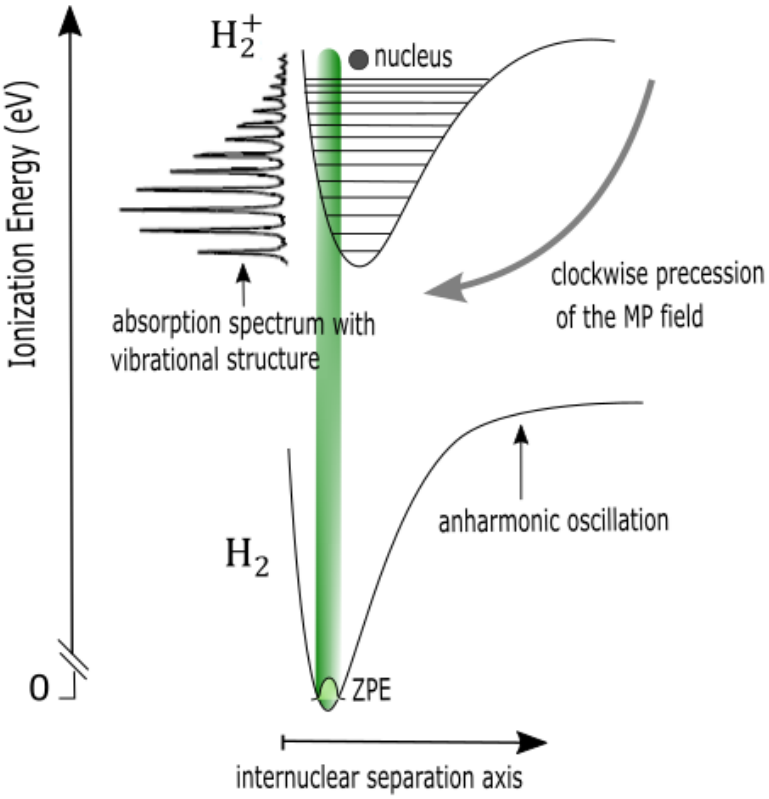

Figure 5. A schematic diagram of the photoelectron spectrum of H_2 molecule [12]. The point-boundary of the so-called zero-point energy (ZPE) is assumed at the 0 position (Fig. 1a). The shift in precession generates anharmonic oscillation. Absorption is quantized along the vibrational states of BOs.

are relatable to the hydrogen oscillator (Fig. 5), where observations at either *x* or *y* directions are referenced to the *z* direction of linear time. The fermion at positions 0 and 2 are aligned with the *z*-axis and positions 1 and 3 are interchangeable with either *x*- or *y*-axes (Fig. 1a). The BOs of a close loop offer quantized energy, $E = nhv$ for the electron's orbit with ZPE at $n = 1$ linked to position 0 (*Postulate 1*). In this way, the *n*-

Preprints (www.preprints.org) | NOT PEER-REVIEWED | Posted: 22 November 2022 doi:10.20944/preprints202210.0172.v3

dimensions of the BOs incorporate the vibrational energy spectrum, $E_n = \left(n + \frac{1}{2}\right)\hbar\omega$, with ω the assumed angular frequency (Fig. 5). The antisymmetric product of one-particle solutions [13] of the Dirac fermion is,

$$\psi(x_1, x_3) = \varphi_1(x_1)\varphi_3(x_3) - \varphi_1(x_3)\varphi_3(x_1)\,. \tag{6a}$$

$$\hat{P}\psi(x_1, x_3) = \varphi_1(x_3)\varphi_3(x_1) - \varphi_1(x_1)\varphi_3(x_3),$$

$$= -\psi(x_1, x_3). \tag{6b}$$

$\hat{p}$ is the probability operator for the Hermitian of the spin 1/2 property of Dirac matrices, $\gamma^{1,3}$ (Fig. 1b). φ is the spinor generated along the BOs into *n*-dimensions of Hilbert space either in outward direction from the precessing MP field or inward direction from the electron's orbit of time reversal. Both are encased by the configurations, Ω of same magnitudes (Fig. 4). These interpretations are applicable to the determination of the fine structures of the hydrogen spectral lines (Fig. 6a–d). Fourier transform is projected in either *x* or *y* directions with reference to *z* direction or intranuclear axis within the atom (Fig. 6a). A hologram sustains unitarity for the dipole moment of the MP field (Fig. 6b). Lorentz transformation of the electron-wave diffraction (Fig. 6c) induces Dirac fermion (Fig. 1a) of an oscillation mode (Fig. 6d) comparable to Fig. 5. How such interpretation translates to a double slit experimentation for entanglement without invoking hidden variables is offered in Fig. 7. Local realism is sustained, where the electron in orbit attains both matter and antimatter features at 720° rotation within the overall spherical rotation of 360° (*Postulate 3*). However, observation at lightspeed is non-deterministic so that

Preprints (www.preprints.org) | NOT PEER-REVIEWED | Posted: 22 November 2022 doi:10.20944/preprints202210.0172.v3

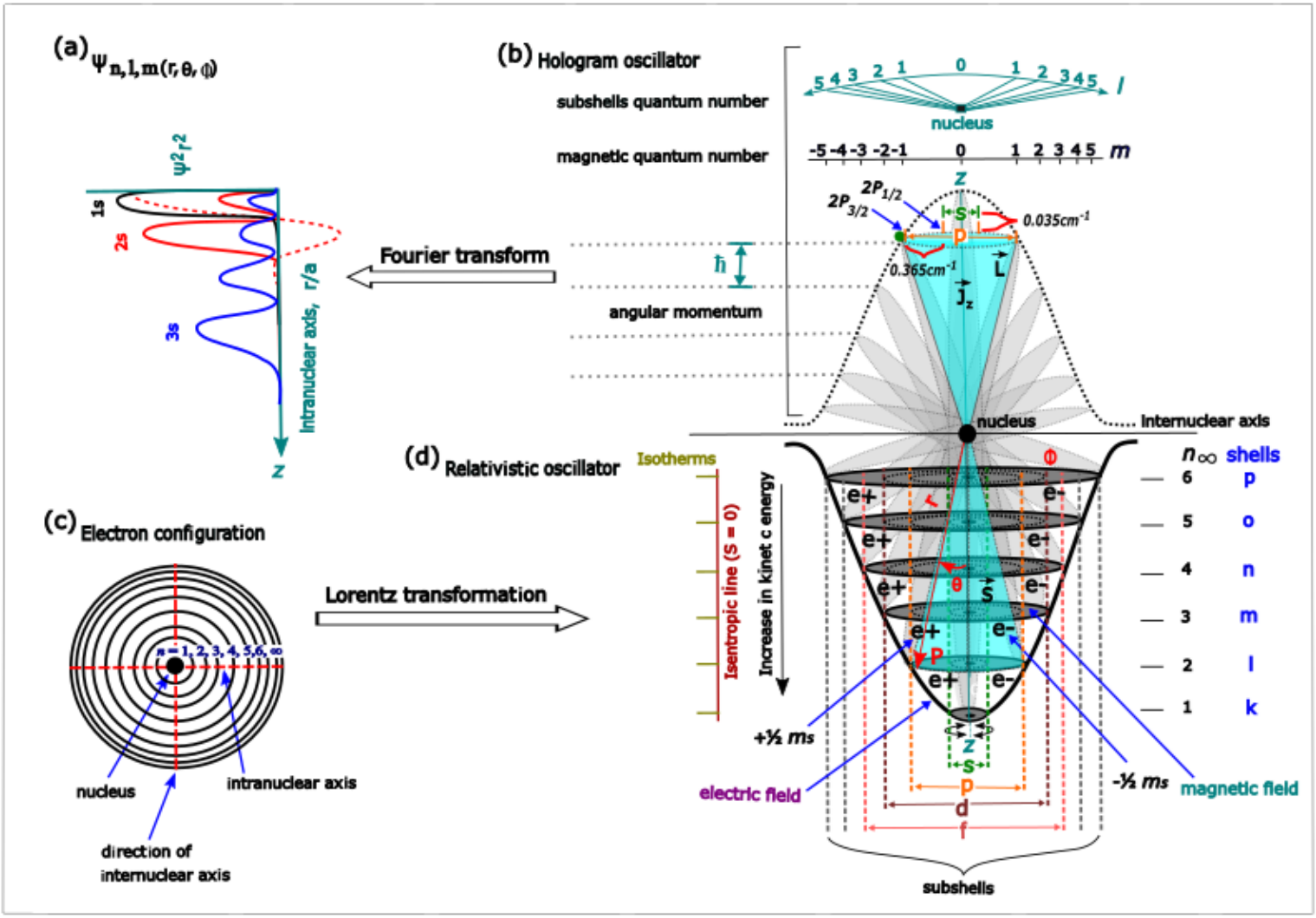

Figure 6. The MP model of the hydrogen atom. (a) Polarization of spin-orbit coupling is referenced to the vertical axis as intranuclear or *z*-axis of linear time. By Fourier transform in 1D space, both radial probability distributions, ψ_{nl} (un-dotted lines) and angular function, ψ_{lm}(red dotted line) for selected orbitals (e.g., 2*s*-orbital) are shown in either *x* or *y* directions (see also Fig. 3a, b and c). (b) A hologram oscillator in comparison to Fig. 4 incorporates both the 3D Schrödinger terms of reference and Dirac theory for spin-orbit splitting [14], i.e., $2P_{3/2}$ and $2P_{1/2}$ at 0.365 cm^{-1} and the lamb shift for $2P_{1/2}$ and $2S_{1/2}$ at 0.035 cm^{-1}. These are applicable to the lone electron (green dot) at position 1 (Fig. 1b), where the transition in its orbit of 4D space-time is defined by $\hbar$ (Fig. 4; *Postulate 1*). (c) Electron configuration

Preprints (www.preprints.org) | NOT PEER-REVIEWED | Posted: 22 November 2022 doi:10.20944/preprints202210.0172.v3

mimicking the electron-wave diffraction and its interaction with light paths energizes the *n*-dimensions of the hydrogen atom perpendicular to the direction of internuclear axis (e.g., Fig. 4). (d) Lorentz transformation for spin-orbit coupling is projected to either *x* or *y* directions with reference to *z* direction in Minkowski space-time (Fig. 1b). Non-commutation, $e^+ \neq e^-$ is applicable to the BOs into *n*-dimensions in violation of lightspeed for local entanglement (*Postulate 1*). The harmonic oscillator is assigned to a classical hemisphere (*Postulate 6*). Cooling and stabilization by external magnetic field generates an isothermal state at the *n*-dimensions. The symbols, *p*, *r*, *θ* and *Φ* (red colored) are referenced to Fig. 4.

Equation 8b is reduced to, $\pm\psi(1/2)$ at positions x_1, x_3 with ± 1 equal to spherical polarization (Fig. 1a). Such intuition is consistent with experiments violating Bell's inequality tests [15, 16]

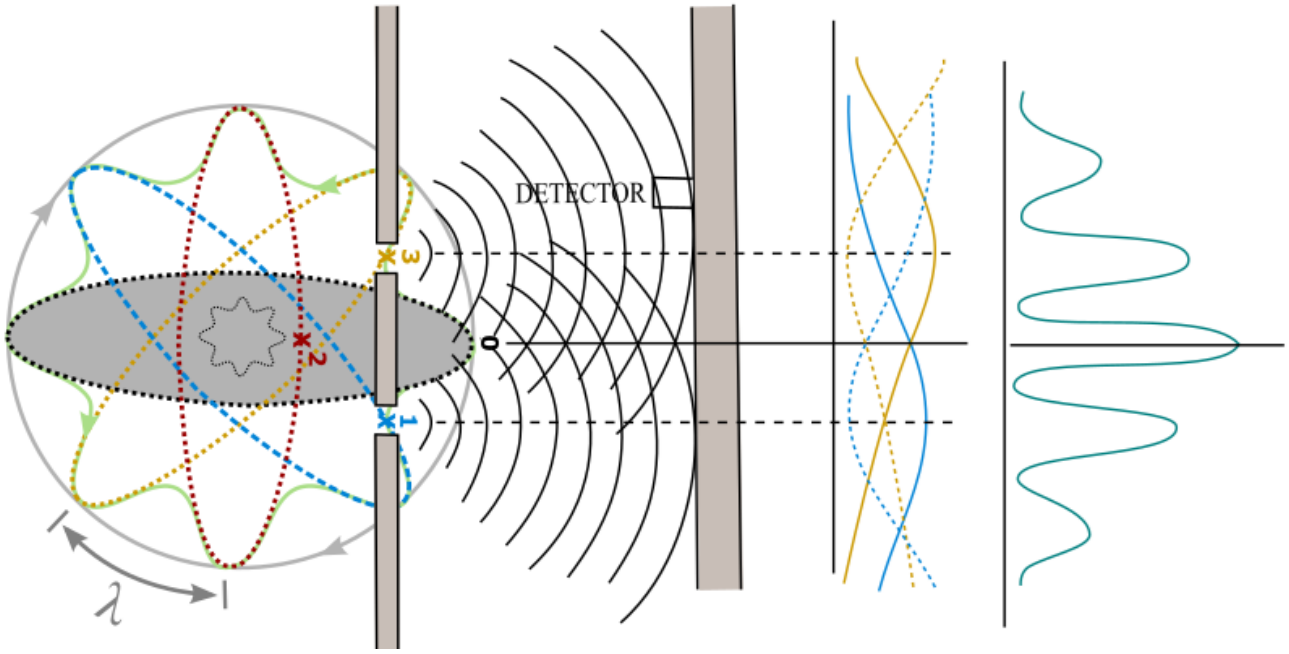

Preprints (www.preprints.org) | NOT PEER-REVIEWED | Posted: 22 November 2022 doi:10.20944/preprints202210.0172.v3

Figure 7. Wave-particle duality of Dirac fermion. The fermion (Fig. 1a) and its wave property are relatable to the double slit experiment for Born's probabilistic interpretation, $|\psi|^2$ by decoherence at observation (*Postulate 3*). The superposition of ±1/2 spins at the pairing positions of 1,5 and 3,7 of BOs for local entanglement (*Postulate 1*) are shown by their respective colored MP fields (Fig. 1a). Multiple slits are also applicable to the BOs of a precessing MP field of a clock face in Hilbert space (e.g., Fig. 2a). Observation is deterministic in 1D space (green wavy curve) comparable to Fourier transform (Fig. 6a). These interpretations are consistent with the Schrödinger's cat narrative and hence, the wave function collapse scenario.

supposing that multielectron are applicable to multiple MP fields (*Postulate 1*) and their interactions with photons could somehow correlate at a distance. The assumption is only applicable to 4D space-time, when observations are reduced to 1D space. The electron's spin is confined to a monopole field of a hemisphere with the outcome of its positive or negative charge depends on whether complete spherical rotation is attained during measurement. From ZPE or vacuum energy at 0 position (Fig. 1a), the transition from $n = 1$ to $n = 2$ accommodates both

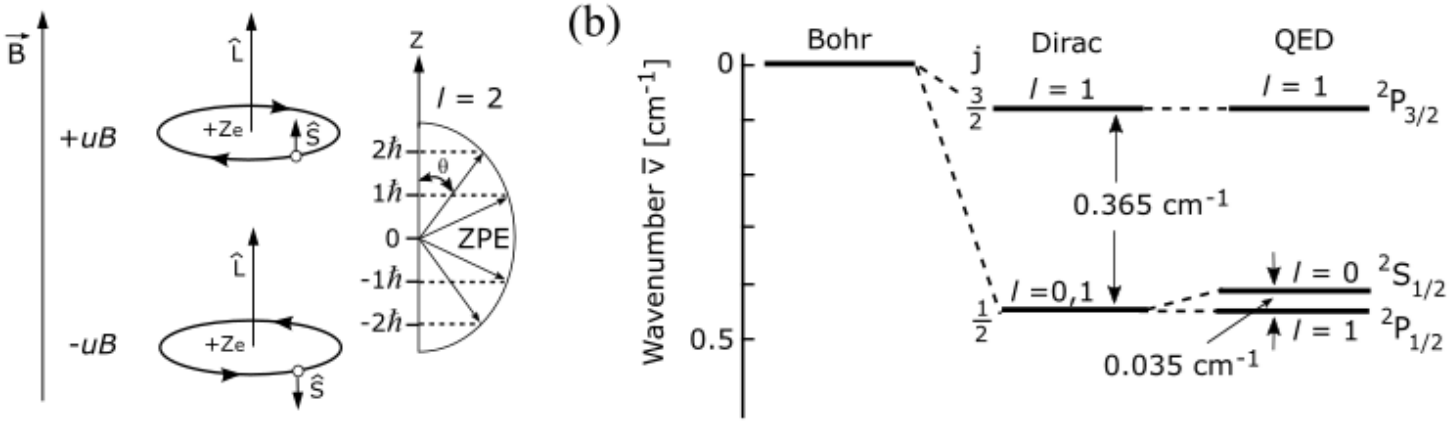

Preprints (www.preprints.org) | NOT PEER-REVIEWED | Posted: 22 November 2022 doi:10.20944/preprints202210.0172.v3

Figure 8. Spin-orbit coupling [11, 14]. (a) In the presence of a weak external magnetic field, $\vec{B}$, its dipole moment, *uB* of classical Bohr magneton exerts corresponding response from the electron's dipole moment. The spin-orbit coupling with reference to either the principal axis of the MP field at position 2 (Fig. 1a) or pairing of positions 2 and 6 (Fig. 1b) is aligned parallel to $\vec{B}$. In this case, ZPE is assumed at position 0. The combined dipole is, $u_z = u_B + u_l$, with u_l equal to $\vec{J}$ and $\vec{J} = l + 1/2$. (b) When *n* = 2, *l* = 1 under unfavorable condition, $2P_{3/2}$ is produced at high energy. In the anticoupling process with $\hat{S}$ in the opposite direction, $2P_{1/2}$ is attained at a low energy. The lamb shift shows that $2S_{1/2}$ is generated probably due to the peak at *n* = 1 (e.g., Fig. 6d).

Dirac spinor and hence, lamb shift for the BOs in degeneracy (Fig. 6b). These are applicable to the conventional interpretation, where total angular momentum, $\vec{J} = l \pm \frac{1}{2}$, provides the values, $\frac{3}{2}$ and $\frac{1}{2}$ for *n* = 2, *l* = 1 (Fig. 8a and b). Supposing that each subshell of an eigenstate possesses spin 1/2 of a light-cone within a hemisphere (Fig. 6d), then $n_2 + n_1 = \frac{3}{2}$ (i.e., 1/2 + 1/2 + 1/2 from the combinations of *s*-*p* subshells for the electron configuration with 1s2s2p assigned). Similarly, $n_2 - n_1 = \frac{1}{2}$ for the *p* subshell is comparable to, 1/2 + 1/2 − 1/2. Due to the peak (Fig. 6b), the *s* subshell attains a slightly higher potential energy than *p* subshell at *n* = 2 (Fig. 8b). The multiplicity of the subshells, i.e., $2\left(S_{\frac{1}{2}}, P_{\frac{1}{2}}\right)$ somehow relates to the 720° rotation before the Dirac fermion assumes its original state. Precession of the MP field allows for changes in *l* and the orientation of the *p* subshells with respect to *m* values (Fig. 6b), while the dipole moment obeys Pauli exclusion principle for the electron distribution (e.g., $1s^2 2s^2 2p^6$). These interpretations are applicable to the Clebsch−Gordon series for the total orbital angular moment, $\vec{L} = \sqrt{l(l+1)}\hbar$ and total spin, $\vec{S} = \sqrt{s(s+1)}\hbar$ at the *n*-dimensions (e.g., Fig. 8a). The lamb shift refines the value of the fine-structure

Preprints (www.preprints.org) | NOT PEER-REVIEWED | Posted: 22 November 2022 doi:10.20944/preprints202210.0172.v3

constant, α to about less than 1 part in a billion [17] and this quantifies the gap between the fine structure of the hydrogen spectral lines with respect to degenerate BOs. It is an indication of the strength of the electromagnetic interaction between elementary charged particles by the relationship,

$$a = \frac{e^2}{4\pi\epsilon_0}, \tag{7}$$

where ε_0 is the vacuum permittivity and e is electron charge. In high-energy physics, a nondimensional system is used with the boundary, ϵ_0= c = $\hbar$ = 1, so Equation 7 becomes,

$$a = \frac{e^2}{\hbar c} \approx \frac{1}{137.036}. \tag{8}$$

No two electrons are present in the hydrogen atom so e^2 relates to the ability of the electron to undergo 720° to form both matter and antimatter, while its transition in orbit of Hilbert space into *n*-dimensions is quantized, $\hbar$ (Fig. 4). The anomalous dipole moment of the electron with respect to its *g*-factor is computed by perturbative expansion to the powers of α in the form,

$$g_e = 2\left(1 + \frac{a}{2\pi} + \cdots\right). \tag{9}$$

Equation 9 simply describes the 720° rotation for the electron as twice the classical spherical rotation at 360° in Hilbert space (Fig. 1a and b). The exponential expansion is related to continual rotation of the electron in orbit. At the present stage, the predicted and measured *g*-factor for the electron is well in agreement to about 10 decimal points [18]. The relationship between the generated magnetic moment, u_s and *g*-factor is,

 doi:10.20944/preprints202210.0172.v3

$$u_s = g_e \frac{u_B}{\hbar} s, \tag{10}$$

where *s* is the intrinsic spin property of the electron. The electron is a classical Bohr magneton, u_B (Fig. 8), where its path is quantized, $\hbar$ (Fig. 4). Unlike a rotating classical object, its spin and intrinsic angular momentum are applicable in Minkowski space-time (Fig. 1b). Thus, by default, the constants, *e*, *c*, *h* and ε_o are naturally integrated into the MP model. Other related themes that can also be pursued perhaps in a similar process include Zeeman effect, quantum Hall effect, Coulomb interactions, Rydberg constant and so forth. In the subsequent section, the implications of these presentations to high-energy physics, general relativity, Dirac spinor and its field theory are briefly examined in order to pave their future research paths from an alternative perspective.

4. The implications

The demonstrations of Dirac fermion and lamb shift in the preceding sections pose a new perspective to the nature of spin-orbit coupling in an atom. Similarly, quantization of the electron's orbit and its wave-particle duality is attained in 4D space-time. Aided by the postulates, the model offers the avenue to explore the possible relationship between quantum mechanics and general relativity from alternative standpoint at the fundamental level. This is complemented by an intuitive demonstration of the Dirac spinor and its field theory.

 doi:10.20944/preprints202210.0172.v3

4.1 The basics of the Standard Model (SM) theory

Yukawa definition for the relativistic range of interaction, $R = \hbar/mc$ adapts the wave-particle duality of the uncertainty principle [19]. Yang-Mills theory of the SM requires, $m = 0$ to sustain unitarity or gauge invariance for conservation in which case, R becomes infinite [20]. Similarly, $m \neq 0$ draws divergent terms to the Fourier Transform integral, $\int d^4k$ with k equal to 4th dimensional variable (Fig. 6a). The Higgs scalar field, Φ of quartic self-interacting terms in the SM lagrangian resolves both glitches of infinity for high-order terms. The theory quite successfully accounts well for the electroweak force. However, further decay of the Higgs boson to observable supersymmetry partners of fermions and bosons presents the hierarchy dilemma of the vacuum state [21]. Conversely, at the nucleus, the property of asymptotic freedom sets the limit for proton mass in terms of quarks in hadrons collisions [22]. This accounts really well for quark confinement and permits, $m = 0$ at long range for the strong nuclear force. Attempts to apply similar process to the mass acquisition scenario of $W^{\pm}$ and Z° bosons other than the Higgs mechanism is pursued by Technicolor theories [23]. But without any new insights offered by experiments, the SM is resigned to the ethos, ‘shut up and calculate’ and this brings into question its completeness to effectively address physics at the fundamental level. Similarly, other features which cannot be accounted for by the SM include quantum gravity, neutrino mass, dark matter and dark energy amongst others. To maneuver through such a hurdle is fairly constrained by conventional methods and this is mostly pursued by superstring theories. The MP model of 4D space-time applied in this study for the Dirac fermion offers one alternative path to examine physics beyond the SM in a probable quantum universe.

Preprints (www.preprints.org) | NOT PEER-REVIEWED | Posted: 22 November 2022 doi:10.20944/preprints202210.0172.v3

4.1.1 Quantum universe

In an atomic universe the electron is a Dirac fermion and it assumes its own antimatter at 720° rotation of a clock face within a classical spherical rotation of 360° in Euclidean space-time (Fig. 1a). By assuming unitarity, the electron removal by ionization is expected to generate particle-hole symmetry for the model. The excitation of the ZPE at position zero is then assumed by the scalar Higgs boson (Fig. 5). Any interactions of the models allow for both vertex corrections and Dirac annihilation process for the spin-orbit coupling at the quantized states of BOs (Fig. 9a). This is applicable to the MP model (Fig. 1a and b) and how this translates to the electric field in Hilbert space is demonstrated in Fig. 2a and b. Suppose Higgs is a heavier version of the Dirac fermion, its four-component spinor field would appear independent of each other at observation by constraining any decaying process. Thus, $H°$ and $Z°$ would translate to ψ^0 and ψ^2 at positions 0 and 2 respectively and $W^{\pm}$ bosons of doublet weak isospin to ψ^1 and ψ^3 at positions 1 and 3 of BOs (*Postulate 3*). Whether these explanations are applicable to the simulation of the Higgs excitation by controlled Raman pulses on non-interacting cold hydrogenic atom of spin-orbit coupling in condensed matter physics [24] is open to further discussions. In this case, the Higgs boson assumes the quantum critical point between the classical and quantum states.

If the model is applicable to the subatomic scale, a proton would assume a triangulated pair for the quark transition in a superfluid state (Fig. 9b) comparable to the Dirac fermion (Fig. 1a). The quark then mimes the four-component Dirac fermion in Euclidean space-time. Superposition states of spin ±1/2 for up or down quark are independently applicable to ψ^1 and ψ^3 at positions 1 and 3 (Fig. 1b; *Postulate 3*). This can somehow relate to the Schrödinger cat narrative of the electron-wave diffraction (Fig. 7). For example, in the

Preprints (www.preprints.org) | NOT PEER-REVIEWED | Posted: 22 November 2022 doi:10.20944/preprints202210.0172.v3

tetraquark model (Fig. 9b), positions 1 and 3 are combined at observation due to confinement unlike Fourier transform

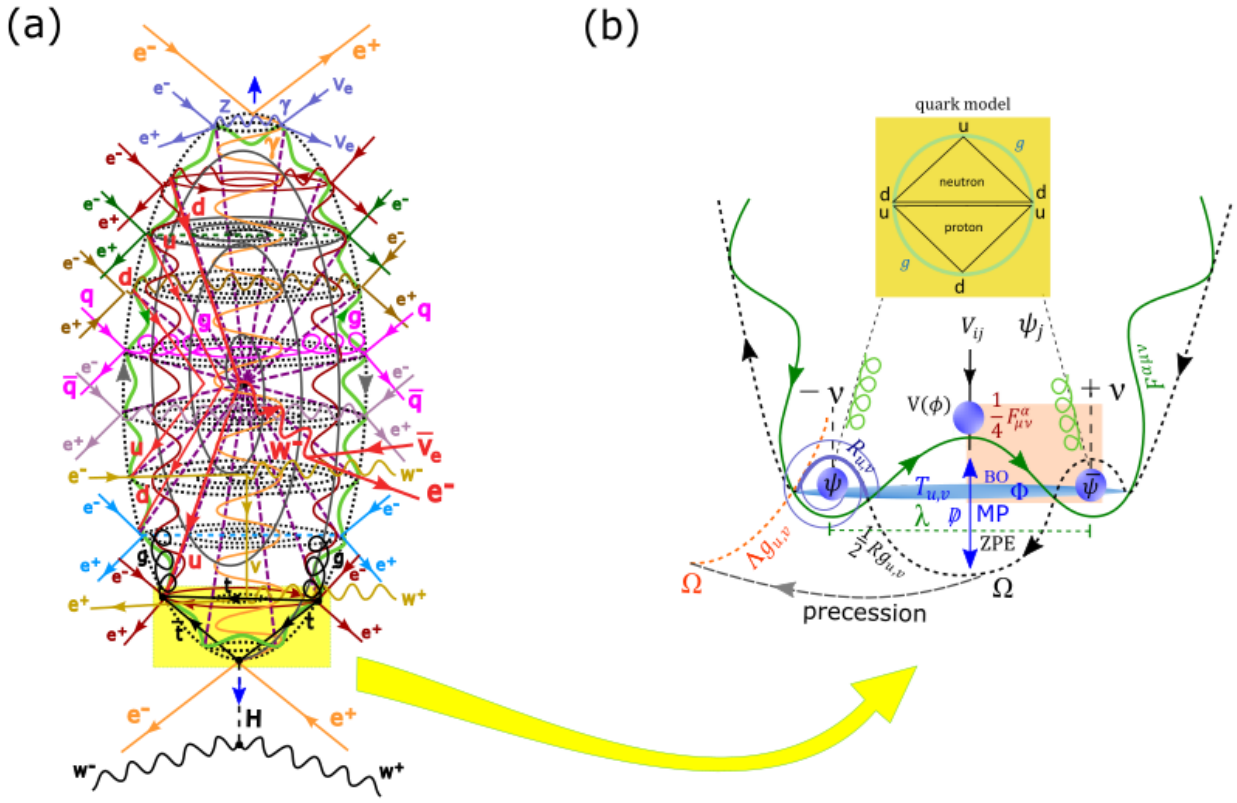

Figure 9. A quantum universe. (a) Quantum foam of vacuum fluctuations. At disturbance, a plethora of particle types is expected at the quantized states of the BOs. The process is analogous to particles popping in and out of existence in accordance with Feynman path integrals. (b) Expansion of the area highlighted in yellow is explored for the Higgs sector. The emergence of the Higgs field of ZPE is somehow related to the electron. The Dirac fermion of four-component spinor (Fig. 1a) is assumed by the Higgs boson (position 0), $W^{\pm}$ bosons (positions 1 and 3) and Z boson (position 2) of time invariant. Observation sustains $\Delta E.\Delta t \geq \hbar/2$ (*Postulate 2*) in accordance with asymptotic freedom (area highlighted in orange). Somehow, this is applicable to free reign of quark in confinement (insert image) within a hemisphere of spin

Preprints (www.preprints.org) | NOT PEER-REVIEWED | Posted: 22 November 2022 doi:10.20944/preprints202210.0172.v3

1/2. So that position 0 is occupied by the up quark and position 2 by down quark. At positions 1 and 3, the quark is in superposition states of weak isospin and is held together by gluons. In this way, both Einstein's terms of general relativity in Euclidean space-time [7] and lagrangian mechanics [25] are intuitively applied to a quantum universe of 4D space-time. See text for brief explanations.

(Fig. 4a) assigned to individual position for the wave function collapse. Thus, the non-abelian gauge group can be either up, down (positive pion, π^+), down, up (π^-), up, up or down, down of opposite charges for neutral (π°) at either position 1 or 3 for Lorentz transformation in Minkowski space-time (Fig. 1b). The rotation of the quark within a hemisphere provides the color charge for the gluons. Any instability of the nucleon would allow for the electroweak nuclear decay like beta decay, $n^\circ \rightarrow p + W^- \rightarrow uud + e^- + \bar{\nu}$, and this reinforces the quark model with e^- representing the overarching Dirac fermion (Fig. 1a and b). The transition between the two universes could account for neutrinos and antineutrinos in Hilbert space (e.g., Fig. 2a).

Suppose the neutron dictates the next triangulate pair in the bottom hemisphere, it will appear invariant to the proton tetraquark model and a pair can somehow incorporate *SU*(3) flavor octet (J = 1/2) and its decuplet (J = 3/2) for the baryon of weak nuclear isospin comparable to the light-cones (Fig. 1b, 4b and d) of Dirac fermion. In this way, asymptotic freedom becomes natural analogous to local realism and entanglement (*Postulate 1*), while observation is deterministic and it violates Bell's inequalities (Fig. 7). Perhaps, the three generations of the quarks and leptons would appear as a function of increasing mass. Similarly, the $W^\pm$ and Z° bosons would relate to spherical rotations of color change of charges, whereas mass acquisition is by oscillation process. These explanations offer the dynamics of the MP model, where many other aspects of particle physics can be explored.

Preprints (www.preprints.org) | NOT PEER-REVIEWED | Posted: 22 November 2022 doi:10.20944/preprints202210.0172.v3

4.1.2 Space-time curvature at the fundamental level

The idea that curved space-time could be fundamental to nature for both matter and the astrophysical universe was first proposed by assuming the existence of an object called geon (gravitational−electromagnetic entity) [26]. The geon concentrates energy and dictates the curvature of space, whereas space tells it how to move analogous to a cosmic black hole. The discrepancy to such novelty is that geon is considered to be a field and by quantum fluctuations of a quantum foamy layer, it is subject to Hawking radiations, where information is lost through time. However, the actual nature of a black hole especially at singularity remains pending in the absence of direct evidences. Likewise, experiments mimicking the Big Bang such as the CERN's large hadrons collider are yet to unveil micro black holes if these actually exist. So we are caught somehow in the middle of time trying to decipher what space-time is actually like either at the initial Big Bang scenario or to glimpse it properly from the overall expansion of the universe. Hence, a refined version of Wheeler's coinage, matter tells space-time how to curve and space-time tells matter how to move to be made fundamental evades conventional methods. But how this could possibly apply to the MP model of 4D space-time is explored in here.

In a quantum universe of a multiverse of the MP models at a hierarchy of scales, Einstein's field terms of space-time geometry [27] can be differentiated from the lagrangian terms of the SM [24] (Fig. 9b). Such a proposition has been made elsewhere for an object field, ψ [7]. In this case, the field tensor, $F_{u,v}$ defines the curvature of the gauge electromagnetic field. Comparably, $R_{u,v}$ is the Ricci curvature tensor of precessing MP field of a clock face induced by the presence of matter. $G_{u,v}$ is a metric tensor of 4D space-time and is

Preprints (www.preprints.org) | NOT PEER-REVIEWED | Posted: 22 November 2022 doi:10.20944/preprints202210.0172.v3

linked to the *n*-dimensions of BOs. It can either contract, $\frac{1}{2}Rg_{u,v}$ by gravity or expand, $\Lambda g_{u,v}$ due to precession in Hilbert space. The stress-energy tensor, $T_{u,v}$ and Dirac notation, $\not{D}$ are incorporated by the BOs into *n*-dimensions (Fig. 1a). Yukawa coupling, V_{ij} links the quark model to the Higgs sector of non-abelian of Lorentz invariance in both Euclidean and Minkowski space-times (Fig. 9b). These explanations purely describe the space-time geometry offered by the MP model, where Newtonian gravity is presumably localized in a universe. The interconnectivity in a multiverse at a hierarchy of scales is possibly provided by the magnetic dipole moment. In this case, whether the Hermitian, $\psi\bar{\psi}$ for the Higgs sector (Fig. 9b) could relate to gravitational waves emanating from the merging of binary black holes [28] is open to further discussions supposing that Higgs boson appears at the singularity of the gauge field defined by ZPE (e.g., Fig. 3). Accelerated expansion of the universe then would mimic precession [7], where time is considerably slowed at the cosmic scale (*Postulate 5*). Observation by constant lightspeed of linear time is redshifted. These explanations are highly speculative but somehow they become relevant to the pursuits of the Big Bang, hierarchy dilemma, neutrino oscillations, quantum gravity, baryon asymmetry, dark matter, dark energy and so forth and they warrant further investigations.

4.2 Quantum Electrodynamics

The MP model of a dipole moment and the emergence of the Higgs amplitude (Fig. 9b) constraints the observations of monopoles as also noted in current experimental undertakings. With this process, both non-relativistic and relativistic aspects of QFT are incorporated into the model. How this becomes relevant to Dirac spinor and its field theory is further explored in this section.

Preprints (www.preprints.org) | NOT PEER-REVIEWED | Posted: 22 November 2022 doi:10.20944/preprints202210.0172.v3

4.2.1 Dirac spinor

Diagonal coupling of rotating BOs and $\vec{L}$ produces intrinsic properties of $\vec{J}$ or the spinor in units of $\hbar$ (Fig. 8a). This is applicable to the reduction of Dirac fermion of four-component spinor field to spin ±1/2 states (Fig. 1b). The pair of light-cones are of time invariant to the helicity of the model. The left-handed helicity is equal to 360° rotation of the fermion or positron between positions, 0 to 3, when the direction of the spin is opposite to direction of motion (Fig. 8a). This is attained within a hemisphere or equivalent to 180° rotation of the overarching spherical model (Fig. 1a and 10). Positive or right-handed helicity is restored at 720° rotation of the fermion or equivalent to 360° spherical rotation, where the electron resumes its original state. The process somehow indicates space inversion or parity transformation of the model through the center from 1 to −1 (Fig. 10). In this way, chiral symmetry is offered by the fermion within a hemisphere,

where the four-component spinor of the Dirac fermion is of unidirectional for the spherical rotation at 360° (Fig. 1a). With these interpretations, it is possible to distinguish between Dirac, Weyl and Majorana fermions and possibly neutrinos. For example, Weyl fermion is assigned to the pair of light-cones of time invariance (Fig. 1b and 10). Each position at 0, 1, 2 and 3 of BOs (Fig. 1a; *Postulate 1*) assumes its own antimatter during the twisting and unfolding process towards 720° rotation compared to 360° rotation at lightspeed and this identifies with Majorana fermion. The electron itself is a Dirac fermion of four-component spinor field (Fig. 1b), while the neutrinos are possibly vibrational manifestations between the Dirac fermion and the quark such as for the electroweak force of beta decay (see subsection 4.1.1). For the broad spectrum of the electromagnetic waves, the classical qubits, 0, −1 and 1 are generated but 0 and 1 dominate (Fig. 10). By combining these

Preprints (www.preprints.org) | NOT PEER-REVIEWED | Posted: 22 November 2022 doi:10.20944/preprints202210.0172.v3

explanations with those offered in the previous section, the possible path for the unification of $U(1)$ x $SU(2)$ symmetry of non-abelian electroweak force is unveiled.

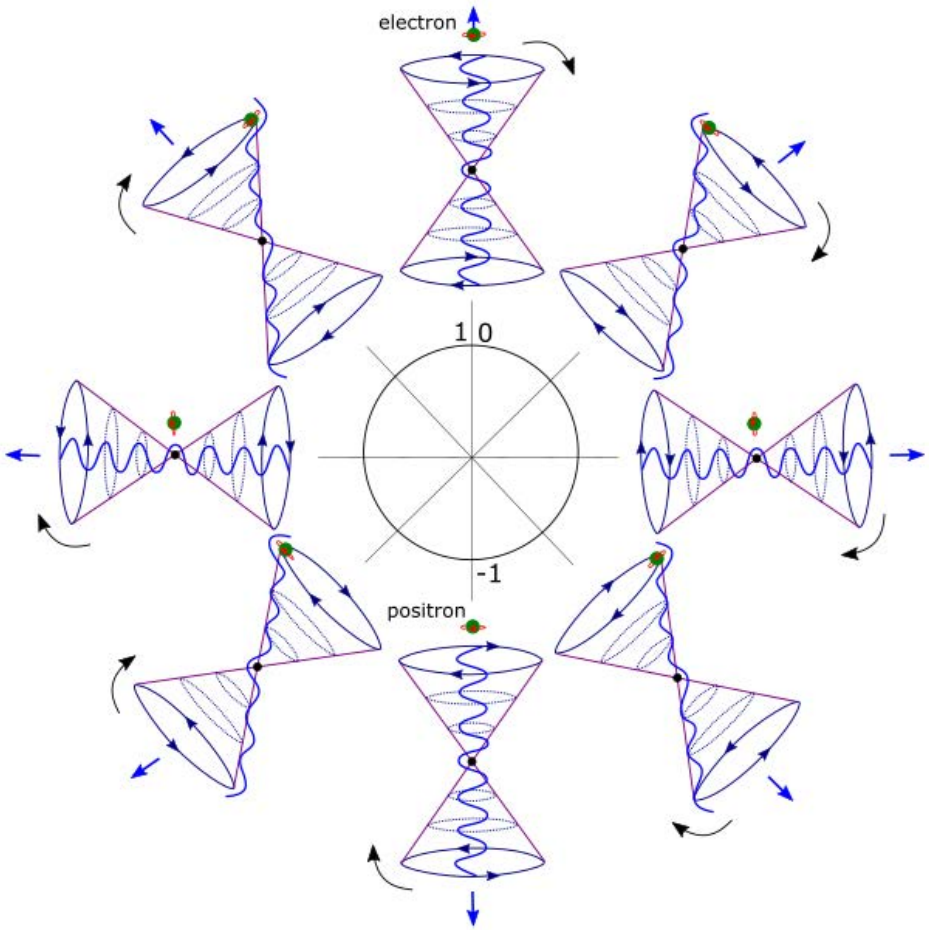

Figure 10. Dirac spinor. The transition of the Dirac fermion in Euclidean space-time (Fig. 1a) to Minkowski space-time (Fig. 1b) is explored for the spin property. The spinor (blue arrows) shows the orientation of the BOs of the light-cones at precession. At 180° spherical rotation of the electron (green dot), spin, +1/2 of negative helicity or −1 qubit is attained, where the direction of spin is opposed to direction of motion. The recoiling (blue wavy curve) of BOs from the unfolding at maximum twist repeats the rotation process to 720° or equivalent to 360° spherical rotation (i.e., qubit 1), where the electron resumes its original state of spin, −1/2 of positive helicity. Similarly, both parity transformation and chirality are also applicable to the quantized electron's orbit (see also Fig. 1a and 2a).

Preprints (www.preprints.org) | NOT PEER-REVIEWED | Posted: 22 November 2022 doi:10.20944/preprints202210.0172.v3

4.2.2 Dirac field theory

The theory is very well developed within the area of quantum electrodynamics with numerous literatures available. In here, certain aspects of the field theory are considered with respect to the intuitive form of the Dirac fermion unveiled in this study (Fig. 1a). Such undertaking is based on a number of selected references [29–31].

⇒ **Maxwell electromagnetism.** The spherical MP model sustains unitarity, *U*(1) symmetry of unidirectional (Fig. 1a), while measurement is of linear time in 1D space (Fig. 3a, b and c). Both are relatable to the classical Maxwell's equation to describe the electron in orbit of the general form,

$$\boldsymbol{\nabla} . \boldsymbol{E}\,(\psi) = -\frac{\partial \boldsymbol{B}}{\partial t}(\psi) = m_j \hbar\,(\psi), \tag{11}$$

where $\boldsymbol{\nabla}$ is the divergence of the dipole moment of the MP field during precession and m_j is the spin momentum. **E** and **B** are orthogonal to each other in space-time (*Postulate* 2) with **B** defined by the BOs in degeneracy (*Postulate 1*). The shift in the electron's position about the BO is given by the Faraday's relationship,

$$\boldsymbol{\nabla} . \boldsymbol{B}\,(\psi) = U_0 J + U_0 \varepsilon_0 \frac{\partial \boldsymbol{E}}{\partial t}(\psi), \tag{12a}$$

so that,

Preprints (www.preprints.org) | NOT PEER-REVIEWED | Posted: 22 November 2022 doi:10.20944/preprints202210.0172.v3

$$\boldsymbol{\nabla} . \boldsymbol{E}\,(\psi) = \frac{\rho}{\varepsilon_0}(\psi). \tag{12b}$$

The density, ρ of the vacuum state (Fig. 9a) is constrained to Ω of spherical configurations, whereas Ω x Ω^* is Hermitian of discrete space-time given by, $\hbar$ (Fig. 9b). The electron's orbit and its interaction from external light offers the qubits, −1, 0 and 1 (Fig. 10) and this can become important to both classical and quantum computing.

⇒ **Dirac field.** Lorentz transformation of the electron to the fermion field of spin ±1/2 is applicable to the MP model. These are denoted $\psi(\mathbf{x})$ in 3D space and $\psi(\mathbf{x},t)$ in both Euclidean and Minkowski space-times (Fig. 1a and b) inclusive of the Higgs sector (Fig. 9b). The Dirac equation for the fermion field is given by,

$$i\hbar\gamma^u\partial_u\psi(x) - mc\psi(x) = 0, \tag{13}$$

where γ^u are the gamma matrices related to the shifts in the electron position of time reversal due to gravity (Fig. 1b). The exponentials of the matrices, $\{\gamma^o\gamma^1\gamma^2\gamma^3\}$ are assigned to positions, 0, 1, 2 and 3 of BOs (Fig. 1a; *Postulate 1*). γ^orelates to arrow of time in asymmetry at position, 0 for a monopole field and $\gamma^1\gamma^2\gamma^3$ variables to Dirac matrices in 3D space (Fig. 1b). These are all incorporated into the famous Dirac equation,

$$\left(i\gamma^0\frac{\partial}{\partial t} + cA\frac{\partial}{\partial x} + cB\frac{\partial}{\partial y} + cC\frac{\partial}{\partial z} - \frac{mc^2}{\hbar}\right)\psi(t,\vec{x}), \tag{14}$$

Preprints (www.preprints.org) | NOT PEER-REVIEWED | Posted: 22 November 2022 doi:10.20944/preprints202210.0172.v3

where the lightspeed, *c* acts on the coefficients A, B and C and transforms them to γ^1, γ^2 and γ^3. Alternatively, the exponentials of γ are denoted *i*, where γ^i is off-diagonal Pauli matrices at γ^1 and γ^3 with respect to the pair of light-cones (Fig. 1b). This is defined by,

$$\gamma^i = \begin{pmatrix} 0 & \sigma^i \\ -\sigma^i & 0 \end{pmatrix}, \tag{15a}$$

and zero exponential, γ^o to,

$$\gamma^0 = \begin{pmatrix} 0 & 1 \\ 1 & 0 \end{pmatrix}. \tag{15b}$$

σ^i is applicable to intersections of the BOs along the electron path for the anticommutation relationship, $e^+(\psi) \neq e^-(\bar{\psi})$ of the Lie algebra group (*Postulate 1*). The matrices, 0 and 1 of Equation 15b is relatable to Fig. 10 and Fig. 2a.

⇒ **Weyl spinor.** The Weyl spinor of the pair of light-cones is applicable to the precessing MP field at the four positions, 0 to 3 of BOs (Fig. 1a; *Postulates 1* and *3*). This is represented as,

$$\psi = \begin{pmatrix} \psi_0 \\ \psi_1 \\ \psi_2 \\ \psi_3 \end{pmatrix}, \tag{16}$$

Preprints (www.preprints.org) | NOT PEER-REVIEWED | Posted: 22 November 2022 doi:10.20944/preprints202210.0172.v3

and they correspond to spin up fermion, a spin down fermion, a spin up antifermion and a spin down antifermion. At 360° rotation, a spin down fermion and its antifermion is assumed. The spin up fermion and its antifermion is restored at 720° rotation (e.g., Fig. 1a and 2a). By relativistic transformation, observation is reduced to a bispinor (e.g., Fig. 7),

$$\psi = \begin{pmatrix} u_+ \\ u_- \end{pmatrix}, \tag{17}$$

where $u_\pm$ are the Weyl spinors of chiral form related to ψ_1 and ψ_3 by vertical projection along the *z*-axis (e.g., Fig. 1b and 6a). These are irreducible within the model. Parity operation $x \rightarrow x' = (t, -\mathbf{x})$ for qubit 1 and −1 (Fig. 2a and 10) along the vertical axis exchanges the left- and right-handed Weyl spinor in the process,

$$\begin{pmatrix} \psi'_L \\ \psi'_R \end{pmatrix} = \begin{pmatrix} \psi_R(x) \\ \psi_L(x) \end{pmatrix} \Rightarrow$$

$$\begin{aligned} \psi'(x') &= \gamma^0 \psi(x) \\ \bar{\psi}'(x') &= \bar{\psi}(x)\gamma^0. \end{aligned} \tag{18}$$

Both left-handed (*L*) and right-handed (*R*) helicities are described in Fig. 10 and 8a with respect to 720° rotation of the electron. The Weyl spinors are converted to Dirac bispinor, ξ^1 ξ^2 diagonally at positions 1 and 3 of BOs (Fig. 1b). Normalization of the two-component spinor, ξ^1 ξ^2 = 1 ensues by the orthogonal relationship, $\begin{pmatrix} 1 \\ 0 \end{pmatrix}$ and $\begin{pmatrix} 0 \\ 1 \end{pmatrix}$ for the full rotation of the sphere (Fig. 10). As mentioned earlier, the Lorentz transformation of matter to antimatter for the Dirac four-component spinor is akin to Majorana fermions (e.g., Fig. 2a). However, these are constrained by observations to

 doi:10.20944/preprints202210.0172.v3

spin, ± 1/2 of linear time (e.g., Fig. 6a and 7). Whether their interactions with external light causes perturbations of the degenerate BOs to generate oscillation modes of neutrino types is open to further discussions, for these would also acquire mass in a similar process.

⇒ **Lorentz transformation.** The Hermitian, $\psi^{\dagger}\psi$ for the Dirac fermion transiting at positions, 0, 1, 2 and 3 of BOs (Fig. 1b) is not Lorentz invariant for measurement of 1D space. These states are in superposition but are deterministic at observations (e.g., Fig. 4a and 7). Weyl spinor of a light-cone depicts the relationship,

$$u^{\dagger}u = (\xi^{\dagger}\sqrt{p.\sigma},\ \xi\sqrt{p.\bar{\sigma}}\,.\begin{pmatrix}\sqrt{p.\sigma}\xi\\ \sqrt{p.\bar{\sigma}}\xi\end{pmatrix},$$

$$= 2E_P\xi^{\dagger}\xi\,. \qquad (19)$$

Equation 19 would relate to 180° spherical rotation while observation is reduced to *z*-axis (e.g., Fig. 2a, 3a and 6a). The corresponding Lorentz scalar of the BOs is,

$$\bar{u}(p) = u^{\dagger}(p)\gamma^{0}, \qquad (20)$$

and is referenced to time axis of the MP field. By identical calculation to Equation 19, the Weyl spinor becomes,

$$\bar{u}u = 2m\xi^{\dagger}\xi, \qquad (21)$$

Preprints (www.preprints.org) | NOT PEER-REVIEWED | Posted: 22 November 2022 doi:10.20944/preprints202210.0172.v3

for the complete rotation of the sphere at 360° (Fig. 2a and 10). Based on the model, it is difficult to distinguish both Weyl spinor and Majorana fermion from the Dirac spinor by relativistic transformation as mentioned earlier (see also subsection 4.2.1).

⇒ **Quantized Hamiltonian.** The 4-vector spinors of Dirac field, $\psi(x)$ offers a level of complexity to observations (Fig. 1a and b). Only two ansatzes to Equation 13 are adapted as follow,

$$\psi = u(\mathbf{p})e^{-ip.x}, \tag{22a}$$

$$\psi = v(\mathbf{p})e^{ip.x}. \tag{22b}$$

These are Hermitian plane wave solutions and they form the basis for Fourier components in 3D space (e.g., Fig. 6a; *Postulate 2*). Decomposition by Hamiltonian then assumes the relationships,

$$\psi(x) = \frac{1}{(2\pi)^{3/2}} \int \frac{d^3}{2E_{\mathbf{p}}} \sum_s \left(a_{\mathbf{P}}^s u^s(p) e^{-ip.x} + b_{\mathbf{P}}^{s\dagger} v^s(p) e^{ip.x} \right), \tag{23a}$$

$$\bar{\psi}(x) = \frac{1}{(2\pi)^{3/2}} \int \frac{d^3}{2E_{\mathbf{p}}} \sum_s \left(a_{\mathbf{P}}^{s\dagger} \bar{u}^s(p) e^{ip.x} + b_{\mathbf{P}}^s \bar{v}^s(p) e^{-ip.x} \right). \tag{23b}$$

The coefficients $a_{\mathbf{P}}^s$ and $a_{\mathbf{P}}^{s\dagger}$ are ladder operators, which are applicable to the BOs into *n*-dimensions along the orbital paths. These are for *u*-type particles and similar process is accorded to $b_{\mathbf{P}}^s$ and $b_{\mathbf{P}}^{s\dagger}$ of *v*-type particles (e.g., Fig. 2a and b). With unitarity sustained, Hilbert space of the

Preprints (www.preprints.org) | NOT PEER-REVIEWED | Posted: 22 November 2022 doi:10.20944/preprints202210.0172.v3

model can undergo both contraction and relaxation with external light interactions, where both types of particles are incorporated. For example, the former is accorded to Einsteinian gravity of time reversal with respect to the center and the latter to overall precession of the MP model of a clock face (e.g., Fig. 2a). The terms, $u^s(p)$ and $v^s(p)$ are Dirac spinors for the two spin states, ±1/2 and $\bar{v}^s$ and $\bar{u}^s$ for their antiparticles. The conjugate momentum is,

$$\pi = \frac{\partial \mathcal{L}}{\partial \psi} - \bar{\psi} i\gamma^0 = i\psi^\dagger. \tag{24}$$

Equation 24 is assumed by the electron in orbit of 3D space against precessing MP field of a clock face in 4D space-time (Fig. 2a). The generated oscillations are of lagrangian mechanics (e.g., Fig. 7b) and its Hamiltonian in 3D space is,

$$H = \int d^3x \psi^\dagger(x)[-i\gamma^0\gamma.\boldsymbol{\nabla} + m\gamma^0]\psi(x). \tag{25}$$

The quantity in the bracket is the Dirac Hamiltonian of one-particle quantum mechanics provided also in Equation 3. With *z*-axis aligned to time axis in asymmetry for a monopole field of a hemisphere (Fig. 6a), the currents are projected in either *x* or *y* directions in 3D space by the relationships,

$$\left[\psi_\alpha(\mathbf{x},t), \psi_\beta(\mathbf{y},t)\right] = \left[\psi_\alpha^\dagger(\mathbf{x},t), \psi_\beta^\dagger(\mathbf{y},t)\right] = 0, \tag{26a}$$

Preprints (www.preprints.org) | NOT PEER-REVIEWED | Posted: 22 November 2022 doi:10.20944/preprints202210.0172.v3

$$\left[\psi_\alpha(\mathbf{x},t),\psi_\beta^\dagger(\mathbf{y},t)\right] = \delta_{\alpha\beta}\delta^3(\mathbf{x}-\mathbf{y}), \tag{26b}$$

where α and β denote the spinor components of the ψ. Both Equations 26a and b are applicable to the Dirac fermion, whereas the Higgs sector at γ^0 or position 0 (Fig. 9b) is not influenced by the Pauli matrices. The ψ independent of time in 3D space obeys the uncertainty principle with respect to position, **p** and momentum, **q**, as conjugate operators (Fig. 4). Their commutation relationship is,

$$\left\{a_{\mathbf{p}}^r, a_{\mathbf{q}}^{s\dagger}\right\} = \left\{b_{\mathbf{p}}^r, b_{\mathbf{q}}^{s\dagger}\right\} = (2\pi)^3\delta^{rs}\delta^3(\mathbf{p}-\mathbf{q}). \tag{27}$$

Equation 27 incorporates both matter and antimatter (Fig. 2a), where observation is of linear time (Fig. 3a, b and c). Thus, a positive-frequency is represented by,

$$\langle 0|\psi(x)\bar{\psi}(y)|0\rangle = \langle 0\,| \int \frac{d^3p}{(2\pi)^3}\frac{1}{\sqrt{2E_{\mathrm{p}}}}\sum_r a_{\mathrm{p}}^r u^r(p)e^{-ipx} \times \int \frac{d^3q}{(2\pi)^3}\frac{1}{\sqrt{2E_{\mathrm{q}}}}\sum_s a_{\mathrm{q}}^{s\dagger}\bar{u}^s(q)e^{iqy}\;|0\rangle. \tag{28}$$

In this way, Dirac strings are constrained by the orthogonal duality of **E** and **B** of the MP model (Fig. 1a and 2a).

⇒ **Further undertakings.** The above interpretations with respect to the Dirac fermion (Fig. 1b) demonstrate the compatibility of the model to QFT application as an approximate intuitive guide to the quantum state. Other related themes that can perhaps be explored in a similar manner include

 doi:10.20944/preprints202210.0172.v3

Fock space and Fermi-Dirac statistics, Bose-Einstein statistics, causality, Feynman propagator, charge conjugation, parity, charge-parity-time symmetry and so forth. In this case, the boundary posed by the model could justify the removal of infinities during renormalization process such as for the perturbation theory to conform to measurements.

5. Conclusion

The intuitive form of the Dirac fermion unveiled within the applied MP model of 4D space-time has far reaching implications. It is able to incorporate both relativistic and non-relativistic wave function comparable to the application of QFTs. The outcomes are shown to pave the path for a quantum universe, where the lagrangian terms of the SM and Einstein field equations are incorporated into a geometric space-time of the model. This assumes a multiverse of the models at a hierarchy of energy scales. Though the approach remains somewhat highly speculative to some extent, it offers new insights into phenomena like the hierarchy problem, monopoles existence, baryon asymmetry and so forth. If considered, this could pave the paths for the pursuits of physics from a different perspective altogether beyond the Standard Model by conventional methods and it warrants further investigations.

Competing financial interests

The author declares no competing financial interests.

References

1. E. Nelson. Derivation of the Schrödinger equation from Newtonian mechanics. *Phys. Rev.* 150(4), 1079 (1966).
2. C. Rovelli. Space is blue and birds fly through it. *Philos. Trans. Royal Soc. Proc. Math. Phys. Eng.* 376(2123), 20170312 (2018).
3. D. H. Perkins. Proton decay experiments. *Ann. Rev. Nucl. Part. Sci.* 34(1), 1-50 (1984).
4. H. Sun. Solutions of nonrelativistic Schrödinger equation from relativistic Klein–Gordon equation. *Phys. Lett. A* 374(2), 116-122 (2009).
5. S. Oshima, S. Kanemaki & T. Fujita. Problems of Real Scalar Klein-Gordon Field. *arXiv preprint hep-th/0512156* (2005).
6. S. D. Bass, A. De Roeck & M. Kado. The Higgs boson implications and prospects for future discoveries. *Nat. Rev. Phys.* 3(9), 608-624 (2021).
7. S. P. Yuguru. Unconventional reconciliation path for quantum mechanics and general relativity. *IET Quant. Comm.* 3(2), 99–111 (2022). https://doi.org/10.1049/qtc2.12034
8. L. S. Weiss et al. Controlled creation of a singular spinor vortex by circumventing the Dirac belt trick. *Nat. Commun.* 10(1), 1-8 (2019).
9. Z. K. Silagadze. Mirror objects in the solar system?. *arXiv preprint astro-ph/0110161* (2001).
10. G. F. Giudice. The dawn of the post-naturalness era. *arXiv preprint arXiv:*1710.07663 (2017).

11. P. Atkins & J. de Paula. *Physical Chemistry*. 9th Edition. Oxford University Press, New York (2010).
12. https://chem.libretexts.org/Courses/Pacific_Union_College/Quantum_Chemistry/10%3A_Bonding_in_Polyatomic_Molecules/10.04%3A_Photoelectron_Spectroscopy
13. A. Szabo & N. S. Ostlund. *Modern quantum chemistry: introduction to advanced electronic structure theory.* Courier Corporation, Massachusetts, USA (1996).
14. H. Haken & H. C. Wolf. *The physics of atoms and quanta: introduction to experiments and theory* (Vol. 1439, No. 2674). Springer Science & Business Media (2005).
15. A. Aspect, P. Grangier, & G. Roger. Experimental realization of Einstein-Podolsky-Rosen-Bohm Gedankenexperiment: a new violation of Bell's inequalities. *Phys. Rev. Lett.* 49(2), 91 (1982).
16. J. W. Pan et al. Experimental entanglement swapping: entangling photons that never interacted. *Phys. Rev. Lett.* 80(18), 3891 (1998).
17. G. Gabrielse et al. New determination of the fine structure constant from the electron g value and QED. *Phys. Rev. Lett.* 97(3), 030802 (2006).
18. D. Hanneke et al. Cavity control of a single-electron quantum cyclotron: Measuring the electron magnetic moment. *Phys. Rev. A* 83(5), 052122 (2011).
19. N. Arkani-Hamed et al. Solving the hierarchy problem with exponentially large dimensions. *Phys. Rev. D* 62(10), 105002 (2000).
20. C.N. Yang & R. Mills. Conservation of isotopic spin and isotopic gauge invariance. *Phys. Rev.* **96**, 191 (1954).
21. P. Higgs. Spontaneous symmetry breakdown without massless bosons. *Phys. Rev.* **145**, 1156 (1966).

22. D. J. Gross. Nobel lecture: The discovery of asymptotic freedom and the emergence of QCD. *Rev. Mod. Phys.* 77(3), 837 (2005).

23. S. Weinberg. Implications of dynamical symmetry breaking. *Phys. Rev. D* 13, 974 (1976).

24. F. J. Huang, Q. H. Chen & W. M. Liu. Higgs-like Excitations of Cold Atom System with Spin-orbit Coupling. *arXiv preprint arXiv:1207.3707* (2012).

25. J. Woithe et al. Let's have a coffee with the standard model of particle physics!. *Phys. Educ.* 52(3), 034001 (2017).

26. C. W. Misner, K. S. Thorne & W. H. Zurek. John Wheeler, relativity, and quantum information. *Phys. Today* 62(4), 40-46 (2009).

27. M. W. Evans et al. Criticisms of the Einstein Field Equation (Vol. 3). Cambridge International Science Publishing (2011).

28. B. P. Abbott et al. GW150914: Implications for the stochastic gravitational-wave background from binary black holes. *Phys. Rev. Lett.* 116(13), 131102 (2016).

29. M. E. Peskin & D. V. Schroeder. *An introduction to quantum field theory*. Addison-Wesley, Massachusetts, USA (1995).

30. L. Alvarez-Gaumé & M. A. Vazquez-Mozo. Introductory lectures on quantum field theory. *arXiv preprint hep-th/0510040* (2005).

31. G. Eichmann. Lectures on Quantization of the Dirac Field (2020) http://cftp.ist.utl.pt/%7Egernot.eichmann/lecture-notes